

# Gaia 1 and 2. A pair of new Galactic star clusters

Sergey E. Koposov,<sup>1,2\*</sup> V. Belokurov,<sup>1</sup> G. Torrealba<sup>1</sup>

<sup>1</sup>*Institute of Astronomy, University of Cambridge, CB3 0HA*

<sup>2</sup>*McWilliams Center for Cosmology, Department of Physics, Carnegie Mellon University, 5000 Forbes Avenue, Pittsburgh, PA 15213, USA*

Accepted XXX. Received YYY; in original form ZZZ

## ABSTRACT

We present the results of the very first search for faint Milky Way satellites in the *Gaia* data. Using stellar positions only, we are able to re-discover objects detected in much deeper data as recently as the last couple of years. While we do not identify new prominent ultra-faint dwarf galaxies, we report the discovery of two new star clusters, Gaia 1 and Gaia 2. Gaia 1 is particularly curious, as it is a massive ( $2.2 \times 10^4 M_{\odot}$ ), large ( $\sim 9$  pc) and nearby (4.6 kpc) cluster, situated  $10'$  away from the brightest star on the sky, Sirius! Even though this satellite is detected at significance in excess of 10, it was missed by previous sky surveys. We conclude that *Gaia* possesses powerful and unique capabilities for satellite detection thanks to its unrivalled angular resolution and highly efficient object classification.

**Key words:** Galaxy: general – Galaxy: globular clusters – Galaxy: open clusters and associations – catalogues – Galaxy: structure

## 1 INTRODUCTION

In 1785, William Herschel introduced “star gauging” as a technique to understand the shape of the Galaxy. Herschel suggested that by splitting the heavens into cells and by counting the number of stars in each, it should be possible to determine the position of the Sun within the Milky Way. Even though he promoted the method as “the most general and the most proper”, Herschel was quick to point out the possibility of strong systematic effects given that different telescopes would probe the skies to different depths. Over the centuries, Herschel’s prophecy of the merit of the technique was confirmed, and most recently, the data from the all-sky surveys such as Two Micron All-Sky Survey (2MASS) (Skrutskie et al. 2006) and Sloan Digital Sky Survey (SDSS) (York et al. 2000) has been used to show off its true power. However, as the telescope-might grew and yet fainter stars were counted, the problem of minute but systematic depth variations blossomed into a major hindrance to studies of the Milky Way structure.

In the Galaxy, the one application that suffers the most from the non-uniform quality of the “star gage” is the search for the faint sub-structures in the stellar halo. Ultra-faint satellites and stellar streams appear as low-level enhancements of the stellar density field and as such can either be destroyed or mimicked by the survey systematics. For example, for a given exposure on a given telescope, a combination of the atmosphere stability, the sky brightness and the im-

age resolution controls the limiting magnitude at which stars can be distinguished from galaxies with certainty. Of these three factors above, only the camera properties are mostly invariant with time, while - as seen from the ground - the sky is constantly changing. Thus, the faint star counts will fluctuate as a function of the position on the sky in accordance with the survey progress. Around the limiting magnitude, the loss of genuine stars due to poor weather conditions is exacerbated by the influx of spurious “stars”, i.e. compact faint galaxies misclassified as stellar objects. At low Galactic latitudes, diffraction spikes, blooming and ghosts produced by bright stars also contribute large numbers of fictitious “stars”. As a result, typically, over-densities of bogus stellar objects caused by misclassified galaxies in galaxy clusters and by artifacts around bright stars outnumber bona-fide satellites by several orders of magnitude.

Today, some 230 years after Herschel’s first attempt, *Gaia*, the European Space Astrometric Mission, as part of the Data Release 1 (DR1), has produced the most precise Star Gage ever (Perryman et al. 2001; Gaia Collaboration et al. 2016a,b). Positions, magnitudes and a wealth of additional information on over a billion sources, as recorded in the *GaiaSource* table, do not suffer from poor weather conditions or dramatic sky brightness variations. Better still, any spurious objects reported by the on-board detection algorithm, are double-checked and discarded after subsequent visits. In terms of the star-galaxy separation, *Gaia* is truly unique. Its angular resolution is only approximately a factor of two worse than the resolution of the WFC3 camera on-board of the HST and *Gaia* can additionally discriminate

\* E-mail: skoposov@cmu.edu

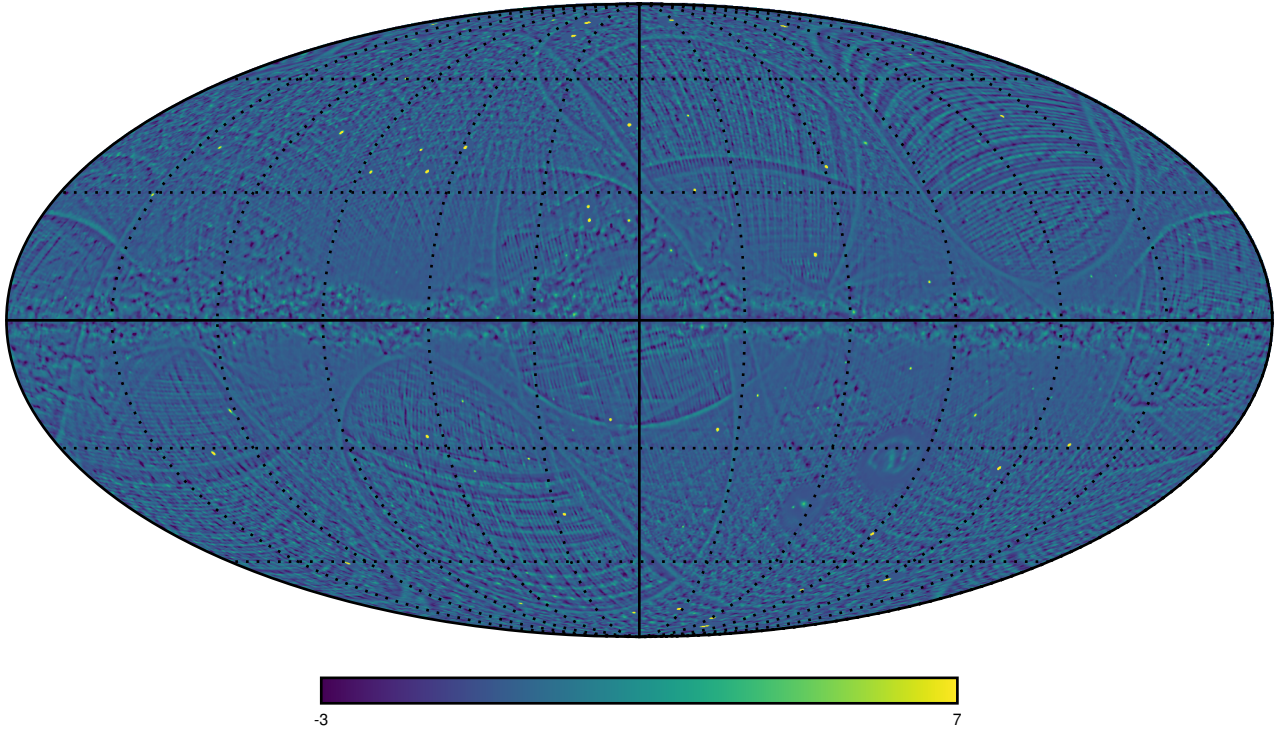


**Figure 1.** The all-sky map of significances of stellar overdensities in Mollweide projection. The map was obtained using a  $12'$  Gaussian kernel.

between stars and galaxies based on the differences in their astrometric behaviour and spectrophotometry. Motivated by the unique properties of the *Gaia* DR1 data, here we investigate the mission’s capabilities for satellite detection. The Paper is organised as follows. Section 2 presents the details of the satellite detection algorithm as applied to the *Gaia* DR1 data. The *Gaia* discoveries are discussed in Section 3. Section 4 studies the properties of the new satellites and Section 5 concludes the paper.

## 2 SATELLITE DETECTION WITH *Gaia* DR1

### 2.1 *Gaia*Source all sky catalogue

The entirety of the analysis presented in this paper is based on the first *Gaia* data product released in late 2016, the *Gaia*Source table. For details on the contents and the properties of this catalogue we refer the reader to the *Gaia* Data Release 1 paper (Gaia Collaboration et al. 2016b). Note that in this paper the only quantities from the catalogue that we use are the stellar positions (RA and Dec), the G-band magnitudes (van Leeuwen et al. 2017) and the values of the `astrometric_excess_noise` parameter (Lindegren et al. 2016).

### 2.2 Satellite search algorithm

The principal ideas behind our Galactic satellite detection algorithm have been extensively covered in the literature (see e.g. Irwin 1994; Belokurov et al. 2007; Koposov et al. 2008a,b; Walsh et al. 2009; Willman 2010; Koposov et al. 2015; Bechtol et al. 2015). However, the *Gaia* DR1 data represents a rather unusual and - in parts - challenging dataset to apply these simply “out of the box”. This is primarily due to the absence of the object colour information, unless, of course, cross-matched with other surveys, which are usually either less deep than *Gaia*, such as 2MASS and APASS or do not cover the whole sky. Additionally, at magnitudes fainter than  $G = 20$ , the survey’s depth starts to vary significantly as a function of the position on the sky. As a result, in this very early data release, the *Gaia* sky appears to look like an intricate pattern of gaps of varying sizes (see e.g. Gaia Collaboration et al. 2016b).

The combination of the factors above drove us to introduce a slight modification to the stellar overdensity identification method. We do use the kernel density estimation with Gaussian kernels of varying width, however in order to assess the significance of the density deviation at any given point on the sky, we do not rely on the Poisson distribution of the stellar number counts. Instead we obtain a local estimate of the variance of the density. More precisely, if  $K(.,.)$  is the properly normalised density kernel on the sphere,  $H(\alpha, \delta)$  is the histogram of the star counts (on HEALPix grid on the sky, Górski et al. 2005), the density estimate is sim-

ply the convolution  $D(\alpha, \delta) = K * H$  and the significance of the overdensity  $S(\alpha, \delta) = \frac{D - \langle D \rangle_A}{\sqrt{\text{Var}_A(D)}}$ , where the average  $\langle D \rangle_A$  and the variance  $\text{Var}_A(D)$  are calculated over the HEALPix neighbourhood (annulus) of a given point. Given the normalisation by local variance, areas with pronounced non-uniformities related to the *Gaia* scanning law, or regions with large changes in extinction are naturally down-weighted in their contribution to significance.

Given that the first *Gaia* DR does not provide colour information, we have to be particularly careful when selecting objects for the satellite search (we cannot use colour-magnitude masks based on stellar isochrones, as in i.e. Koposov et al. 2015). For the analysis in this paper we apply only two selection cuts. First cut concerns the *Gaia*  $G$  magnitude:  $17 < G < 21$ . The reason for getting rid of bright stars, i.e. those with  $G < 17$  is twofold. First, for absolute majority of interesting targets at reasonable distances from the Sun we expect the luminosity function of their stellar populations to rapidly rise with magnitude at  $G > 17$ . Therefore, in these satellites (globular clusters and dwarf galaxies), the number of stars fainter than  $G = 17$  should vastly overwhelm the number of bright stars. Instead, the brighter magnitudes are dominated by the foreground contamination. Equally important is the fact that most (or all) satellites with significant populations of stars at  $G < 17$  have likely been already detected, either through studies of the 2MASS photometry (e.g. Koposov et al. 2008b) or via the inspection of the archival photographic plate data (see e.g. Whiting et al. 2007).

The cut at faint magnitudes  $G < 21$  is less straightforward. Usually, when dealing with large optical ground-based surveys, it is advisable to restrict the data to be limited by the apparent magnitude which gives the most uniform density map. However, in our case, due to the relatively shallow *Gaia* DR1 depth in combination with the rising stellar luminosity function for objects of interest, the benefits of going to e.g.  $G = 21$  as compared to  $G = 20.5$  outweigh the drawbacks of dealing with non-uniform density distribution, caused by spatially varying incompleteness (see e.g. Gaia Collaboration et al. 2016b). Accordingly, for our analysis we set the faint limit at  $G = 21$ .

The second and final cut applied to the catalogue concerns the star/galaxy separation. While the *Gaia*'s on-board detection algorithm was designed with point sources in mind, the observatory nonetheless detects (and reports) compact galaxies at faint magnitudes as well as compact portions of extended galaxies. In fact, in the high latitude ( $|b| > 30^\circ$ ) area where *Gaia* overlaps with the SDSS, at magnitude  $G = 20$  around 10% of sources detected by *Gaia* and reported in the *GaiaSource* catalogue are classified by the SDSS as galaxies (bear in mind though that the SDSS star-galaxy classification is not 100% correct). As galaxies are much more clustered than stars, it is crucial to filter them out from the sample before embarking on the search for over-densities. In the *GaiaSource* catalogue, the parameter which correlates the most with the object's non-stellarity is the `astrometric_excess_noise` metric which measures the extra scatter in the astrometric solution of all objects (Lindgren et al. 2016). Here, in order to reject extended sources in the magnitude range  $17 < G < 21$  we adopt the following magnitude-dependent cut on the `astromet-`

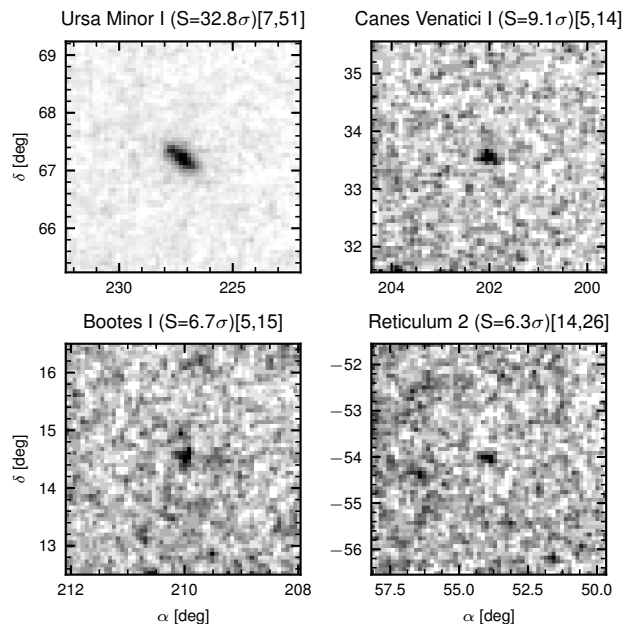


**Figure 2.** The gallery of known faint and ultra-faint Milky Way satellites. The greyscale shows the density of *Gaia* sources with  $17 < G < 21$  and satisfying the stellarity selection (Eq. 1). The significance of the detection of each object is shown in the title. The number of stars per bin corresponding to white and black colour in the density maps is given in brackets in the panel titles.

`ric_excess_noise` parameter:

$$\log_{10}(\text{astrometric\_excess\_noise}) < 0.15(G - 15) + 0.25 \quad (1)$$

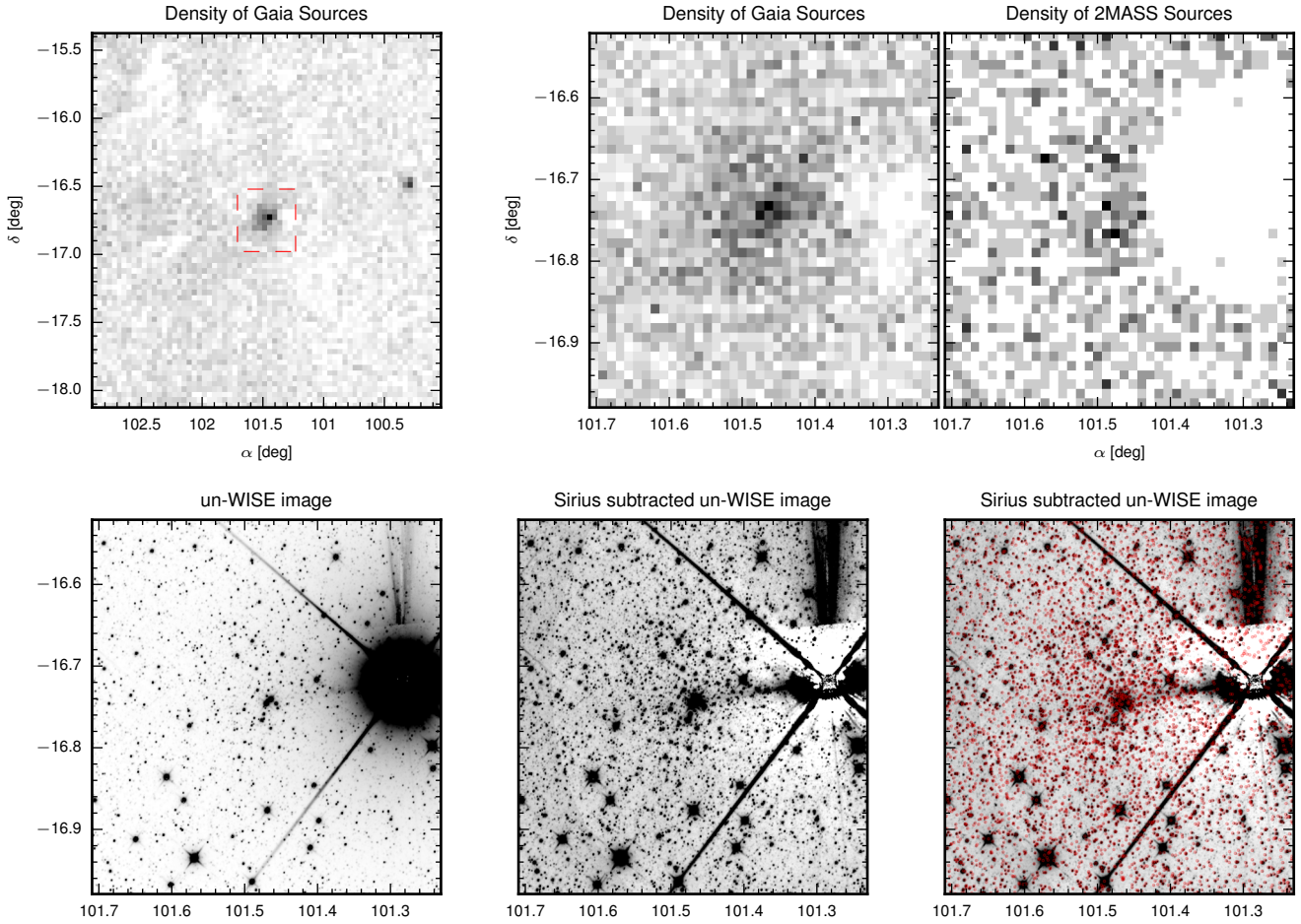
The quality of this selection can be assessed using the SDSS catalogue: in the magnitude range  $19 < G < 20$ , more than 95% of *Gaia* sources rejected by the above cut are classified by SDSS as galaxies confirming that this is indeed a very effective way to weed out spurious “stars” from the *Gaia* stellar sample.

Figure 1 shows the map of significances of overdensities as measured using the Gaussian kernel with  $\sigma = 12'$ . This map is produced using the entire *GaiaSource* catalogue filtered with the cuts described above. Note the compact yellow spots, the vast majority of which correspond to the overdensities associated with the known Galactic satellites. The underlying fine web of green-blue filaments is related to the *Gaia* scanning law.

### 3 DETECTED OBJECTS

#### 3.1 Known objects

In this paper, we choose to focus only on the most obvious detections, i.e. those above  $6\sigma$  in significance. From the suite of runs of the overdensity detection algorithm with different kernels ranging from  $1.5'$  to  $24'$ , a total of 259 such candidates were identified. At the next step, these were cross-matched with various catalogues of star clusters and nearby galaxies (Dias et al. 2002; Kontizas et al. 1990; McConnachie 2012; Harris 2010; Makarov et al. 2014) as well as the CDS's Simbad database (Wenger et al. 2000). Out of the 259 objects, 244 had a clear association with a known star cluster or



**Figure 3.** Distribution of sources around Gaia 1. *Top left:* The density of all *Gaia* sources with  $G < 20$  within  $\sim 3$  degrees of Gaia 1. The overdensity on the right edge of the panel is Berkeley 25, an old open cluster. The red box indicates the size of the region shown on other panels of the figure. *Top middle:* The density of *Gaia* sources with  $G < 20$  in the  $\sim 30' \times 30'$  field of view around Gaia 1. *Top right:* The density of the 2MASS sources in the same field of view. *Bottom left:* The  $30' \times 30'$  image from the WISE survey showing Gaia 1. *Bottom middle:* The same image with the PSF of Sirius subtracted. *Bottom right:* The same image with *Gaia* source positions overlaid in red.

a galaxy. To our surprise the list of previously known satellites detected in the *Gaia* DR1 data at high significance was not limited to the classical globular clusters and the classical dwarf galaxies, known for decades. Amongst the detections, we found several ultra-faint dwarf galaxies, such as Canes Venatici I (Zucker et al. 2006), detected at significance of  $9.1 \sigma$ , Bootes I (Belokurov et al. 2006) detected at  $6.7 \sigma$ , and Reticulum 2 (Koposov et al. 2015; Bechtol et al. 2015) with significance of 6.3. Some other, fainter dwarfs such as Canes Venatici II (Belokurov et al. 2007) and Crater 2 (Torrealba et al. 2016) were also detected, albeit at slightly lower significance (below our nominal threshold), i.e. 5.8 and 5.1 respectively.

Figure 2 shows the density distributions of stellar sources around some of the dwarf galaxies detected in *Gaia* DR1. These range from one of the most prominent dwarfs, namely UMi, to the notoriously difficult to find ultra-faints,

**Table 1.** Measured parameters of clusters detected in *Gaia* dataset

Name	Gaia 1	Gaia 2
Right Ascension [deg]:	101.47	$28.124 \pm 0.007$
Declination [deg]:	-16.75	$53.040 \pm 0.005$
Galactic longitude [deg]	202.34	131.909
Galactic latitude [deg]	-8.75	-7.764
Half-light radius[']:	$6.5 \pm 0.4$	$1.90^{+0.4}_{-0.34}$
Half-light radius[pc]:	$9 \pm 0.05$	$3^{+0.63}_{-0.53}$
Ellipticity:	—	$0.18^{+0.2}_{-0.12}$
Distance modulus (m-M):	$13.3 \pm 0.1$	$13.65 \pm 0.1$
Age [Gyr] <sup>1</sup> :	$6.3 \pm 1$	$8 \pm 2$
Absolute magnitude (V):	$-5 \pm 0.1$	$-2 \pm 0.1$

several of which were detected less than two years ago in the Dark Energy Survey data (Koposov et al. 2015; Bechtol et al. 2015). These examples demonstrate the incredible purity and quality of the *GaiaSource* catalogue, and highlight

<sup>1</sup> Due to limited colour magnitude information, we consider ages highly uncertain



*Gaia*'s superb satellite discovery capabilities even without colour information.

While exploring the candidate over-density list, we have stumbled upon two previously unknown objects detected with very high significance, which are going to be the focus of the rest of the paper.

### 3.2 Gaia 1. You can not be Sirius!

The first stellar overdensity without an obvious counterpart, i.e. without an entry in any of the clusters/galaxies catalogues available to us, has an estimated significance of  $\sim 10$ . Note however, that initially, this candidate, dubbed here Gaia 1, was rejected as it is located in close proximity of the brightest star on the sky – Sirius<sup>2</sup>. Figure 3 shows the distribution of sources in the area around the candidate from three different surveys: *Gaia*, 2MASS and WISE (Wright et al. 2010). As the Figure demonstrates, the overdensity in *Gaia*-detected sources is indeed very prominent (top left and top middle panels). Note a white patch corresponding to a dearth of *Gaia* sources near the centre of the over-density. This is the location of Sirius, where *Gaia* struggles to detect genuine stars<sup>3</sup>. The area affected by Sirius is much larger in the 2MASS data, as evidenced in the right panel. However, even here, a stellar overdensity corresponding to the candidate in question is noticeable. The object itself can be seen directly in the images from the infrared WISE survey (bottom row). The bottom panels of Figure 3 show the view of the  $\sim 30' \times 30'$  area around the overdensity as provided by the un-WISE project (Lang 2014). The left panel displays the original WISE data with Sirius in the picture, while the middle panel has the star subtracted using a circularly symmetric PSF model. In both cases the overdensity of sources in the central parts of Gaia 1 is clearly visible. This is the most straightforward and the most secure confirmation of the newly identified satellite.

Our next step is to try to assess the nature of the overdensity by means of studying its colour-magnitude diagram properties. Unfortunately, the *Gaia* DR1 release does not contain colour information, so we are forced to use much shallower 2MASS data. Left panel of Figure 4 shows the extinction-corrected Hess diagram obtained by combining 2MASS and *Gaia* photometry for the field centred on the Gaia 1 (to get the combined 2MASS/*Gaia* photometry we used the nearest neighbour cross-match between surveys with  $3''$  aperture). The red giant branch together with prominent red clump (or red horizontal branch) at  $K_s \sim 11.7$  are both clearly visible. The other two panels of the Figure show the 2MASS-only colour magnitude diagrams (CMD). The middle panel gives the CMD of the stars within the central parts of Gaia 1 together with the PARSEC isochrone (Bressan et al. 2012) with  $[\text{Fe}/\text{H}] = -0.7$

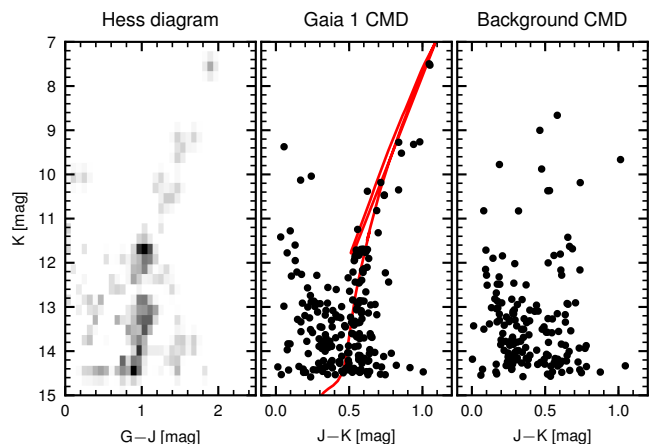


**Figure 4.** *Left panel:* The background subtracted and extinction corrected 2MASS-*Gaia* Hess diagram of the central  $0.1^\circ$  of Gaia 1 (area within the annulus with inner and outer radii of 0.3 and 1 degrees has been used for background); *Middle panel:* The 2MASS  $J - K_s, K_s$  colour-magnitude diagram of Gaia 1 obtained using sources within 0.1 deg from Gaia 1 centre. The PARSEC isochrone with the age of 6.3 Gyr and  $[\text{Fe}/\text{H}] = -0.7$  at the distance modulus of  $m - M = 13.3$  is overplotted in red. *Right panel:* The colour-magnitude diagram of the background field offset by  $0.5^\circ$  from Gaia 1 and with the same area as used for the middle panel.

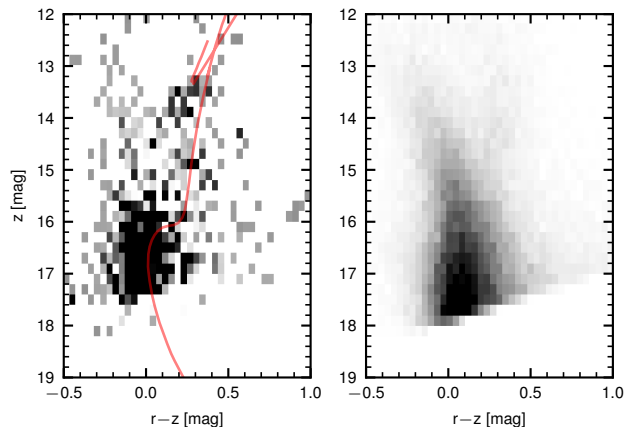


**Figure 5.** *Left panel:* The background subtracted  $r - z, z$  Hess diagram of the central  $0.1^\circ$  of Gaia 1 from PS1 data. The PARSEC isochrone with the age of 6.3 Gyr and  $[\text{Fe}/\text{H}] = -0.7$  at the distance modulus of  $m - M = 13.3$  is overplotted in red. *Right panel:* The Hess diagram of the stellar foreground in the  $0.3^\circ, 1^\circ$  annulus around Gaia 1.

<sup>2</sup> Previously when working with ground-based surveys such as SDSS, VST and DES the authors usually automatically excluded the regions around bright stars as CCD saturation, ghost reflections and diffraction spikes produced by bright stars usually lead to spurious overdensities in the catalogues.

<sup>3</sup> It is curious that in the *Gaia* paper on source list creation by Fabricius et al. (2016) the region around Sirius was used to demonstrate challenges of dealing with such a bright source (see their Fig. 12)

and age of 6.3 Gyr. The right panel of the Figure displays the colour-magnitude distribution of the foreground stars in the part of the sky 0.5 degrees away from the centre of Gaia 1 with the same area as the field shown in the middle panel. We note that the isochrone reproduces the location of the red clump and the red giant branch and that the colour-magnitude distribution in Gaia 1 is clearly different from the distribution of the foreground stars, which provides another confirmation that the object is a genuine satellite.

A better idea of the object’s stellar populations can be gleaned from the recently released Pan-STARRS1 (PS1) data (Chambers et al. 2016; Magnier et al. 2016a,b). Due to the presence of an extremely bright star nearby, the quality of the PS1 data in the region is significantly compromised but the catalogues remain immensely useful. We obtain a list of sources around Gaia 1 from the stack detections catalogue (the `StackObjectThin` table) and require that the sources have the following flags: `STACK_PRIMARY`, `PSFMODEL`, `FITTED` on, and do not have the `SKY_FAILURE` flag. This together with the cut on extinction-corrected r-band magnitude of  $r < 17.5$  provides a relatively clean source subset and allows us to finally peer at the deeper colour-magnitude diagram of the satellite. Left panel of Figure 5 shows the  $r-z$  vs  $z$  extinction corrected (Schlafly & Finkbeiner 2011) background subtracted Hess diagram, while the Hess diagram of the foreground stellar population is displayed on the right. With the PS1 data being deeper compared to 2MASS, we can see the large number of turn-off stars at  $r-z \sim 0$  and  $z \sim 16$ . Note, that these are exactly the stars that contributed most of the signal in the *Gaia* overdensity detection. The PS1 data also shows the RHB (or the red clump) at  $r-z \sim 0.3$ . As the Figure indicates, the 6.3 Gyr and  $[\text{Fe}/\text{H}] = -0.7$  isochrone also provides a decent description of the PS1 data.

### 3.3 Gaia 2

The second object in our list possesses a significance of  $9\sigma$ . This overdensity is located in dense stellar field of the sky, close to the galactic plane at  $b = -8.7^\circ$ . Figure 6 shows an array of discovery plots confirming that the candidate is indeed a *bona-fide* satellite. The left panel of the Figure gives the density distribution of the *Gaia* sources with  $G_0 < 19$  (where  $G_0$  is the extinction-corrected *Gaia* G-magnitude) and `astrometric_excess_noise`  $< 5$ . Here we use the Schlegel et al. (1998) dust map and the extinction coefficient of 2.55 (see Belokurov et al. 2017). It is clear that *Gaia* has detected a pronounced stellar overdensity in the centre of the field. The next panel gives the density distribution of the 2MASS sources and here, similarly to Gaia 1 we see an overdensity at lower significance. The middle right panel displays the colour mosaic of the Digital Sky Survey (DSS) (Blue/Red) images of the area. Note an agglomeration of stars clearly visible in the centre of the image. The rightmost panel presents the dust extinction distribution as reported by the Planck satellite (see Planck Collaboration et al. 2014). While some spatial variation of extinction is noticeable in the area, including a small decrease in reddening in the very centre of the field, there exists no correlation between the dust distribution and the *Gaia* stellar density distribution. Thus, based on the evidence listed above, we conclude that this overdensity is also a genuine Galactic satellite, named Gaia 2 hereafter.

Figure 7 gives a glimpse of the colour-magnitude distribution of the stars in Gaia 2. The 2MASS-based Hess diagram (left) assuredly exhibits the red-giant branch with a possible red clump. Note that both of these CMD features are clearly absent in the foreground population (right panel of the Figure). For Gaia 2, we also utilise the PS1 data to obtain a deeper colour-magnitude diagram of the object. Accordingly, Figure 8 shows the background subtracted and

extinction corrected Hess diagram of the central parts of the Gaia 2 in the PS1 data, while the right panel displays the background Hess diagram; both panels use the  $g$  and  $i$  bands. The depth of the PS1 data is sufficient to see the main sequence (MS) of the satellite. The presence of the obvious MS is the final confirmation of the nature of this stellar overdensity.

## 4 PROPERTIES OF GAIA 1 AND 2

### 4.1 Gaia 1

The extinction-corrected photometry of the satellite as supplied by 2MASS and PS1 is relatively shallow, thus limiting our ability to accurately measure the system’s age, metallicity and distance. However the problem is remedied to some degree by the presence of the obvious Red Clump, visible in the colour-magnitude diagram discussed above, that allows robust distance determination. The 2MASS extinction corrected K magnitude of the Red Clump of Gaia 1 is  $K_s = 11.7$  (with a statistical uncertainty less than 0.01 mag). Although the absolute magnitude of the Red Clump might depend weakly on the age and the metallicity of the stellar population, we assume  $M_K = -1.6$  (see Williams et al. 2013; Girardi 2016, and discussion there). This gives us a distance modulus of  $m - M \sim 13.3 \pm 0.1$  corresponding to  $\sim 4.6 \pm 0.2$  kpc (assuming a systematic uncertainty of  $\sim 0.1$  on the red-clump absolute magnitude). With the distance estimate in hand we can now constrain the age and the metallicity of the system by fitting isochrones to the data. Here we do not try to carry out the full stellar population modelling, due to the limitations of the data currently available. We simply point out that the 6.3 Gyr and  $[\text{Fe}/\text{H}] = -0.7$  isochrone at the distance dictated by the red clump magnitude appears to describe well both the 2MASS red giant branch and the main sequence turn-off visible in the PS1 data (see Figures 4 and 5). We estimate that the age uncertainty is  $\sim 1-2$  Gyr and the uncertainty in  $[\text{Fe}/\text{H}]$  is  $\sim 0.2$  dex.

As a next step we proceed with the determination of structural parameters. Due to the proximity of Sirius and possible spatially variable incompleteness in the catalogue at faint magnitudes, we have decided to use only stars with  $G < 19$  and located far enough from Sirius ( $\alpha > 101.4^\circ$ ). For the same reason, instead of doing the 2-D density analysis we perform an un-binned 1-D density profile fitting using the Plummer model for the satellite and the uniform background density. Table 1 gives the results of the fit together with their uncertainties as determined from 1-D posteriors, which were sampled using the `emcee` ensemble sampler (Foreman-Mackey et al. 2013). Figure 9 shows the Gaia 1’s observed 1D density profile together with our best-fit Plummer model. We note that innermost point of the density profile is deviating slightly from the model, and that the 2-D stellar distribution in Gaia 1 seems to have a rather compact group of stars in the very centre (see top middle panel of Figure 3). We are not able, at this point, to determine the exact cause of this over-density, or even to rule out an artefact unambiguously. The satellite’s half-light radius determined from the fit is  $6.5' \pm 0.4$  which corresponds to  $\sim 9$  pc. Based on the size typical for globular clusters in the MW, we conclude that Gaia 1 is a star cluster, most likely of globular variety

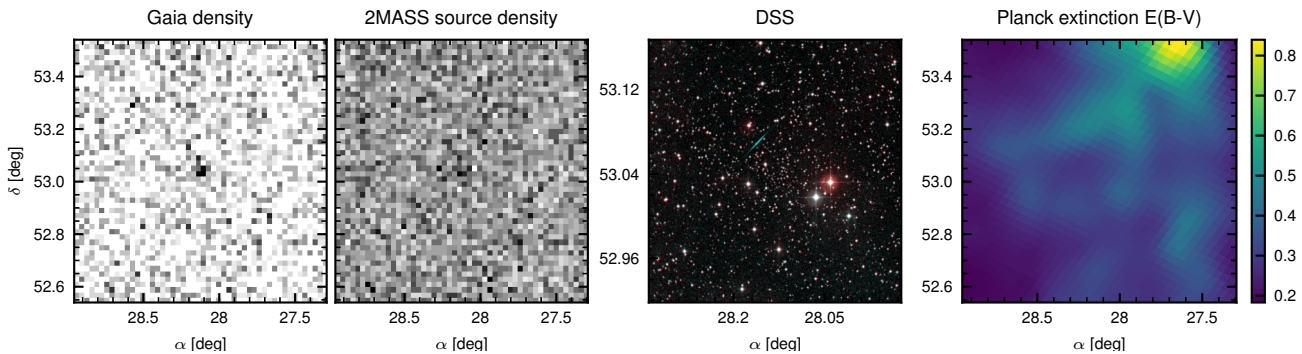


**Figure 6.** *Left panel:* The density of *Gaia* sources with extinction corrected *Gaia* magnitude brighter than 19 in the  $1^\circ \times 1^\circ$  area around *Gaia* 2. *Second panel:* The density of 2MASS sources around *Gaia* 2. *Third panel:* The colour DSS image of  $15' \times 15'$  field of view around *Gaia* 2. *Fourth panel:* The extinction map around *Gaia* 2.

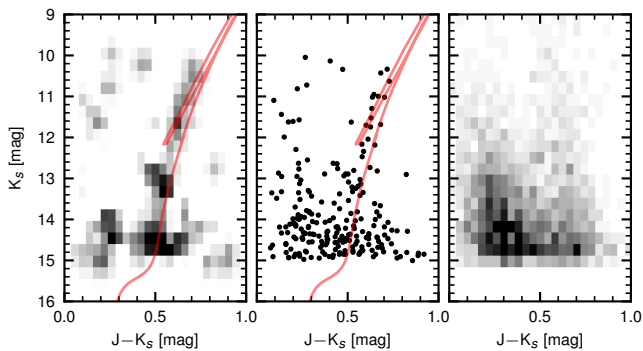


**Figure 7.** *Left panel:* The background subtracted and extinction corrected 2MASS Hess diagram of *Gaia* 2 within central  $3'$ . The PARSEC isochrone with the age of 8 Gyr and  $[\text{Fe}/\text{H}] = -0.6$  at a distance modulus of 14.65 is overlaid in red. *Middle panel:* The 2MASS colour-magnitude diagram of *Gaia* 2 within  $3'$  of centre. *Right panel:* The Hess diagram of the background stars in the  $12'$ ,  $24'$  annulus.

given its age and metallicity. It also could be an old open cluster similar to e.g. Berkeley 25 located only  $\sim 1$  degree away on the sky from *Gaia* 1. From the density profile fit we also determine the total number of the satellite's stars with  $G < 19$ ,  $N \sim 1200 \pm 120$ . Assuming the Chabrier IMF (Chabrier 2003) and the best-fit isochrone, we deduce the total stellar mass of  $22000 M_\odot$  and the  $V$ -band luminosity of  $M_V \sim -5 \pm 0.1$ . Note though that these numbers are only ball-park estimates due to the uncertain age and metallicity of the stellar population.

To investigate the cluster's orbital properties, it would be interesting to gauge the proper motion of the *Gaia* 1's stellar members. Unfortunately, due to the proximity to Sirius, the bright *Gaia* 1 members are not present in the TGAS catalogue, so in order to make a proper measurement we likely have to wait for the second release of *Gaia* data.

## 4.2 *Gaia* 2

The properties of the *Gaia* 2's stellar population, namely its metallicity and age can be deduced from the combination of the 2MASS and PS1 photometry. However, because the PS1 data is limited to the lower Main Sequence, this analysis is

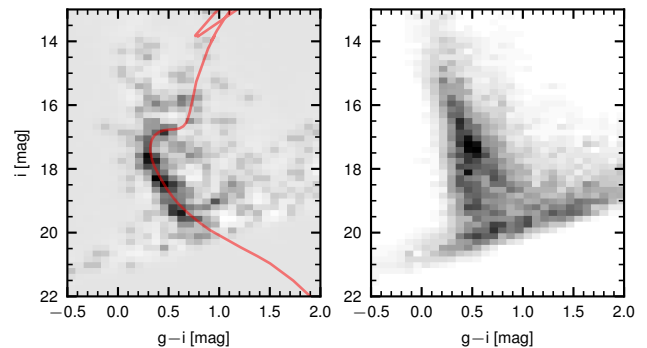


**Figure 8.** *Left panel:* The background subtracted and extinction corrected PS1 Hess diagram of *Gaia* 2 within central  $3'$ . The PARSEC isochrone with the age of 8 Gyr and  $[\text{Fe}/\text{H}] = -0.6$  at a distance modulus of 14.65 is overlaid in red. *Right panel:* The Hess diagram of the background stars in the  $12'$ ,  $24'$  annulus.

subject to a substantial age-metallicity degeneracy. Through experiments with PARSEC isochrones, we find that the stellar population with 8 Gyr and  $[\text{Fe}/\text{H}] = -0.6$  fits both the lower Main Sequence in PS1 and the Red Giant Branch in 2MASS. We estimate the age uncertainty to be  $\sim 1 - 2$  Gyr and metallicity uncertainty  $\sim 0.2$  dex. The distance modulus implied by this isochrone is  $m - M = 13.65 \pm 0.1$  corresponding to the distance of 5.4 kpc. A better imaging is definitely required to make a more detailed determination of the age, metallicity and distance of this object.

To measure the structural parameters of *Gaia* 2 we model the distribution of the *GaiaSource* number counts. We restrict the sample to stars with  $G_0 < 19$ . The spatial density distribution is then modelled with a combination of a flat background and an elliptical Plummer profile for the satellite (for more details see e.g. Koposov et al. 2015). The resulting measurements are given in the Table 1. We find that the object is mildly elliptical, although at low significance levels. The half-light radius of the object is  $\sim 1.9'$ , which at the distance of 5.4 kpc corresponds to 3 pc. Thus, *Gaia* 2 is almost three times smaller compared to *Gaia* 1. The total luminosity of the cluster can be estimated similarly to that of *Gaia* 1 using the best-fit isochrone and the total number of stars with  $G_0 < 19$ , resulting in  $M_V = -2 \pm 0.1$ . Given its size, metallicity, age and appearance on the image

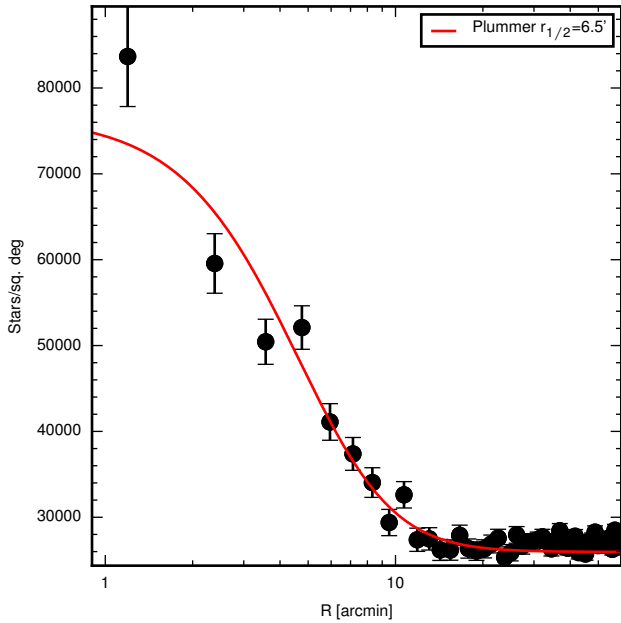


**Figure 9.** The 1D density profile of Gaia 1. The red line shows a Plummer model fit with half-light radius of  $6.5'$ . We also note that in the very centre there is a tight group of stars which causes the innermost point in the density profile to deviate from Plummer.

cutouts, it is most likely a globular cluster, or an old open cluster.

## 5 CONCLUSIONS

This paper presents the results of the very first exploration of the *Gaia* capabilities for Galactic satellite detection. While we have identified a number of new interesting satellite candidates, here we describe only two objects, Gaia 1 and Gaia 2, whose nature can be determined unambiguously with extant data. Possessing remarkably high levels of significance - in excess of 9 (!) - both were, nevertheless, missed by previous imaging surveys. Thus, *Gaia* appears to offer a unique view of the Galactic stellar distribution, unrivalled even by datasets reaching to significantly fainter magnitudes. It is due to the combination of the *Gaia*'s high angular resolution and the high purity of its stellar sample, objects like Gaia 1 can be discovered.

Gaia 1 is a large and luminous star cluster. However, it is positioned almost exactly behind Sirius, the brightest star in the sky, which appears to be the perfect hiding place even for a satellite of such grand prominence. Countless generations of astronomers must have stared right at Gaia 1, blissfully unaware of its existence. The area around Sirius is difficult to analyse as it is littered with artifacts spawned by this extremely bright star. However, given the *Gaia*'s multi-epoch data-stream, such artifacts can be weeded out in the preparation of the *GaiaSource* catalogue. Each time *Gaia* looks at Sirius, the spurious sources appear in different positions on the sky compared to the previous visits and thus are mostly discarded due to the DR1 requirement of having 5 or more detections of a single source (Lindegren et al.

2016). Even if some spurious sources make it to the final *GaiaSource* catalogue, they can be identified very efficiently based on their unusual astrometric behaviour.

We have demonstrated that the *Gaia* data can be used to detect classical dwarf galaxies, ultra faint dwarfs and star clusters in a wide range of sizes and luminosities. All of these are detected with ease using the *Gaia*'s stellar positions only in the catalogue which is known to suffer from spatially-variable incompleteness. We therefore predict with confidence, that in the future *Gaia* Data Releases, when the completeness is stabilised and the colour, distance and proper motion information is added, many new galactic satellites will be revealed.

## ACKNOWLEDGEMENTS

We acknowledge the usage of the HyperLeda database (<http://leda.univ-lyon1.fr>). This research has made use of the SIMBAD database, operated at CDS, Strasbourg, France. The research leading to these results has received funding from the European Research Council under the European Union's Seventh Framework Programme (FP/2007-2013)/ERC Grant Agreement no. 308024. SK thanks the United Kingdom Science and Technology Council (STFC) for the award of Ernest Rutherford fellowship (grant number ST/N004493/1). SK also thanks Bernie Shao for the assistance with obtaining the Pan-STARRS1 data. The authors thank the anonymous referee for careful reading of the manuscript.

This paper was written in part at the 2016 NYC Gaia Sprint, hosted by the Center for Computational Astrophysics at the Simons Foundation in New York City.

This research made use of *Astropy*, a community-developed core Python package for Astronomy (*Astropy* Collaboration et al. 2013) and Q3C extension for PostgreSQL database (Koposov & Bartunov 2006).

This work has made use of data from the European Space Agency (ESA) mission *Gaia* (<http://www.cosmos.esa.int/gaia>), processed by the *Gaia* Data Processing and Analysis Consortium (DPAC, <http://www.cosmos.esa.int/web/gaia/dpac/consortium>). Funding for the DPAC has been provided by national institutions, in particular the institutions participating in the *Gaia* Multilateral Agreement.

The Pan-STARRS1 Surveys (PS1) and the PS1 public science archive have been made possible through contributions by the Institute for Astronomy, the University of Hawaii, the Pan-STARRS Project Office, the Max-Planck Society and its participating institutes, the Max Planck Institute for Astronomy, Heidelberg and the Max Planck Institute for Extraterrestrial Physics, Garching, The Johns Hopkins University, Durham University, the University of Edinburgh, the Queen's University Belfast, the Harvard-Smithsonian Center for Astrophysics, the Las Cumbres Observatory Global Telescope Network Incorporated, the National Central University of Taiwan, the Space Telescope Science Institute, the National Aeronautics and Space Administration under Grant No. NNX08AR22G issued through the Planetary Science Division of the NASA Science Mission Directorate, the National Science Foundation Grant No. AST-1238877, the University of Maryland, Eotvos Lorand



University (ELTE), the Los Alamos National Laboratory, and the Gordon and Betty Moore Foundation.

## REFERENCES

- Astropy Collaboration, Robitaille, T. P., Tollerud, E. J., et al. 2013, *A&A*, 558, A33
- Bechtol, K., Drlica-Wagner, A., Balbinot, E., et al. 2015, *ApJ*, 807, 50
- Belokurov, V., Zucker, D. B., Evans, N. W., et al. 2006, *ApJ*, 647, L111
- Belokurov, V., Zucker, D. B., Evans, N. W., et al. 2007, *ApJ*, 654, 897
- Belokurov, V., Erkal, D., Deason, A. J., et al. 2017, *MNRAS*, 466, 4711
- Bressan, A., Marigo, P., Girardi, L., et al. 2012, *MNRAS*, 427, 127
- Chabrier, G. 2003, *PASP*, 115, 763
- Chambers, K. C., Magnier, E. A., Metcalfe, N., et al. 2016, [arXiv:1612.05560](https://arxiv.org/abs/1612.05560)
- Dias, W. S., Alessi, B. S., Moitinho, A., & Lépine, J. R. D. 2002, *A&A*, 389, 871
- Fabrizius, C., Bastian, U., Portell, J., et al. 2016, *A&A*, 595, A3
- Foreman-Mackey, D., Hogg, D. W., Lang, D., & Goodman, J. 2013, *PASP*, 125, 306
- Gaia Collaboration, Prusti, T., de Bruijne, J. H. J., et al. 2016, *A&A*, 595, A1
- Gaia Collaboration, Brown, A. G. A., Vallenari, A., et al. 2016, *A&A*, 595, A2
- Girardi, L. 2016, *ARA&A*, 54, 95
- Górski, K. M., Hivon, E., Banday, A. J., et al. 2005, *ApJ*, 622, 759
- Harris, W. E. 2010, [arXiv:1012.3224](https://arxiv.org/abs/1012.3224)
- Irwin, M. J. 1994, *European Southern Observatory Conference and Workshop Proceedings*, 49, 27
- Koposov, S., & Bartunov, O. 2006, *Astronomical Society of the Pacific Conference Series*, 351, 735
- Koposov, S., Belokurov, V., Evans, N. W., et al. 2008, *ApJ*, 686, 279-291
- Koposov, S. E., Glushkova, E. V., & Zolotukhin, I. Y. 2008, *A&A*, 486, 771
- Koposov, S. E., Belokurov, V., Torrealba, G., & Evans, N. W. 2015, *ApJ*, 805, 130
- Kontizas, M., Morgan, D. H., Hatzidimitriou, D., & Kontizas, E. 1990, *A&AS*, 84, 527
- Lang, D. 2014, *AJ*, 147, 108
- Lindegren, L., Lammers, U., Bastian, U., et al. 2016, *A&A*, 595, A4
- van Leeuwen, F., Evans, D. W., De Angeli, F., et al. 2017, *A&A*, 599, A32
- Magnier, E. A., Chambers, K. C., Flewelling, H. A., et al. 2016, [arXiv:1612.05240](https://arxiv.org/abs/1612.05240)
- Magnier, E. A., Sweeney, W. E., Chambers, K. C., et al. 2016, [arXiv:1612.05244](https://arxiv.org/abs/1612.05244)
- Makarov, D., Prugniel, P., Terekhova, N., Courtois, H., & Vauglin, I. 2014, *A&A*, 570, A13
- McConnachie, A. W. 2012, *AJ*, 144, 4
- Perryman, M. A. C., de Boer, K. S., Gilmore, G., et al. 2001, *A&A*, 369, 339
- Planck Collaboration, Abergel, A., Ade, P. A. R., et al. 2014, *A&A*, 571, A11
- Schlegel, D. J., Finkbeiner, D. P., & Davis, M. 1998, *ApJ*, 500, 525
- Schlafly, E. F., & Finkbeiner, D. P. 2011, *ApJ*, 737, 103
- Skrutskie, M. F., Cutri, R. M., Stiening, R., et al. 2006, *AJ*, 131, 1163
- Torrealba, G., Koposov, S. E., Belokurov, V., & Irwin, M. 2016, *MNRAS*, 459, 2370
- Walsh, S. M., Willman, B., & Jerjen, H. 2009, *AJ*, 137, 450
- Wenger, M., Ochsenbein, F., Egret, D., et al. 2000, *A&AS*, 143, 9
- Whiting, A. B., Hau, G. K. T., Irwin, M., & Verdugo, M. 2007, *AJ*, 133, 715
- Williams, M. E. K., Steinmetz, M., Binney, J., et al. 2013, *MNRAS*, 436, 101
- Willman, B. 2010, *Advances in Astronomy*, 2010, 285454
- Wright, E. L., Eisenhardt, P. R. M., Mainzer, A. K., et al. 2010, *AJ*, 140, 1868-1881
- York, D. G., Adelman, J., Anderson, J. E., Jr., et al. 2000, *AJ*, 120, 1579
- Zucker, D. B., Belokurov, V., Evans, N. W., et al. 2006, *ApJ*, 643, L103

This paper has been typeset from a  $\text{\TeX}/\text{\LaTeX}$  file prepared by the author.